On-the-fly Acquisition and Rendering with Low Cost Lidar and RGB Cameras for Marine Navigation

Somnath Dutta[1][a], Fabio Ganovelli[1][b] and Paolo Cignoni[1][c]

[1] *Institute of Information Science and Technologies "Alessandro Faedo" (ISTI), Italian National Research Council (CNR), Via Giuseppe Moruzzi 1, 56124 Pisa, Italy*
{firstname.lastname}@isti.cnr.it

Keywords: LIDAR-RGB images calibration, Computer Graphics

Abstract: This paper describes a hardware/software system, dubbed NausicaaVR, for acquiring and rendering 3D environments in the context of marine navigation. Like other similar work, it focuses on system calibration and rendering but the specific context poses new and more difficult challenges for the development when compared to the classic automotive scenario. We provide a comprehensive description of all the components of the system, explicitly reporting on encountered problems and subtle choices to overcome those, in an attempt to render an insightful picture of how this and similar systems are built.

1 INTRODUCTION

The proliferation of high-quality depth sensors and cameras at an affordable price has enriched the domain of graphics and vision and consequently resulted in the development of advanced applications covering broad disciplines. Among those applications, there is a certain proportion that intends to present information to the user in an elementary fashion and specifically related to the situation and environment. Cameras have been the predominant choice for a visual navigational system, however, with the increasing availability of depth sensors, the geometric understandings added an extra dimension to the entire visual navigational ecosystem.
Marine navigation, often subjected to adverse weather and lighting conditions, has traditionally relied on the intensive manual labor of its crew. Alike land or aerial navigational systems, cameras are the preferable choice and are now augmented with 3D sensors, for instance, Lidars. Traditionally, marine vessels, for instance, ships and boats, relied on manual intervention for maneuvering in harbor areas and face the risk of collisions with the docked ships(or boats) causing damages to both sides. A dearth of qualitative visual perception of the surroundings and the associated controls account for some of the major fatalities and cost-intensive repairs.
An intelligent system with a feature for displaying a realistic environment of the surroundings for smart maneuvering in marine vessels mandates the integration of multi-modal sensors. An accurate and realistic resemblance of the environment is indispensable for obstacle detection and especially for guaranteeing emergency services overseen by the intervention of onboard personnel. A holistic system that offers multi-modal sensor support, distributed deployment focusing on a data-flow model between the sensors and central system server, video stream, information transmission, and finally remote access between onshore and offshore participants is essential for e-navigation technology and could be used as real industry products.
With the above-mentioned objective in focus, we highlight the substantial outcomes of our work as summarized below.

- a testbed architecture with multiple cameras and low-cost lidar sensors, described in section 3.1
- an ad hoc method (section 4) for registration of input data in a common reference frame

The paper is organized into multiple sections focusing on related works in section 2, a description of the overall system-cum-architecture in section 3 followed by calibration of lidars and cameras in section 4. Finally, section 5 is dedicated to the real-time acquisition and rendering with the conclusion of our work in section 6.

[a] https://orcid.org/0000-0003-3982-8780
[b] https://orcid.org/0000-0002-0378-9188
[c] https://orcid.org/ 0000-0002-2686-8567

2 RELATED WORK

Visual sensors play a key role in maneuvering operations for diverse scenarios, for instance, street navigation with automotive vehicles (Li et al., 2020), aerial navigation (Paneque et al., 2022) with drones and marine operations (Kim et al., 2020) in boats and ships. In recent years, technologies such as sensing devices, Artificial Intelligence (AI), and the Internet of Things (IoT) have made rapid progress and are frequently used in numerous fields. In the field of marine vessels, research & development of technology-related autonomous ships (Schubert et al., 2018), (Hahn et al., 2022) has been actively carried out globally to improve safety by preventing human error and improving working conditions by reducing the workload on crew. SmartKai (dspace, 2021) is an application-oriented research & development project that focused on a parking system for ships at the harbor based on lidar sensors. The project includes developing a smart user interface so that ship crews can easily visualize navigation data on varieties of display platforms. In (Snyder et al., 2004), a camera-based visual sensing system is proposed to cater to maritime navigation and reconnaissance system for multiple applications, for instance, obstacle avoidance, and area survey analysis.

(Rüssmeier et al., 2016) conceptualized and implemented an experimental maritime testbed for the design and evaluation of sensor data fusion, communication technology, and data stream analysis tools. The author considered the entire setup to be highly flexible and can be applied in various research fields, from e-navigation to the generation of situational awareness. A maritime physical testbed/cyber-physical system (LABSKAUS) (Brinkmann and Hahn, 2017) provides various maritime-specific components such as a reference waterway, research boat, and mobile bridge. Furthermore, an architecture consisting of a data model, message parser, wireless infrastructure, and a polymorphic interface offering integration of various prototype designs is proposed as part of LABSKAUS. (Martelli et al., 2021) discuss digitalization in marine vessels as a significant process directed toward autonomous navigation, cost reduction, safety, and reliability. The authors point out that the complete system consisting of advanced sensors, Artificial Intelligence, and alternative display techniques (VR, AR) is a major requirement in the marine intelligent system, but also pitches an enormous challenge for integration and deployment. (Perera et al., 2012) proposed a simple hardware system and software architecture for collecting the sensor data (non-visual) targeting autonomous surface vessels (ASVs). Furthermore, a human-machine interface (HMI) is implemented as part of the system.

A chronological trend of the ASVs existing autonomy levels in marine vessels and multi-agent control architecture from the perspective of ASVs is presented in (Schiaretti et al., 2017). According to the authors, situation awareness that forms an integral block of the navigation systems heavily relies on sensor fusion and the corresponding data visualization. (Thombre et al., 2022) presents a detailed review of the sensor and AI technique for environment perception and awareness for autonomous ships. (Wright, 2019) explores the use of AI techniques to integrate multiple sensor modalities into a cohesive approach for autonomous ship navigation. The use of multiple redundant sensors overcomes the limitation and vulnerabilities of the individual sensor and the usage of advanced learning methodology addresses key areas of detection and identification providing comprehensive situational awareness to be effective in real-time maneuvering.

Our paper reflects on a complete framework based on low-cost sensors, unlike existing methodology inherently addresses the problem of registering/calibrating multi-modal data especially plagued by low-resolution, sparsity of lidar data and importantly, the environment. We elaborate on the alignment of the multi-modal data in section 4 taking into allowance the above-mentioned difficulties using a combination of customized calibration objects and minimal algorithmic steps.

3 SYSTEM AT A GLANCE

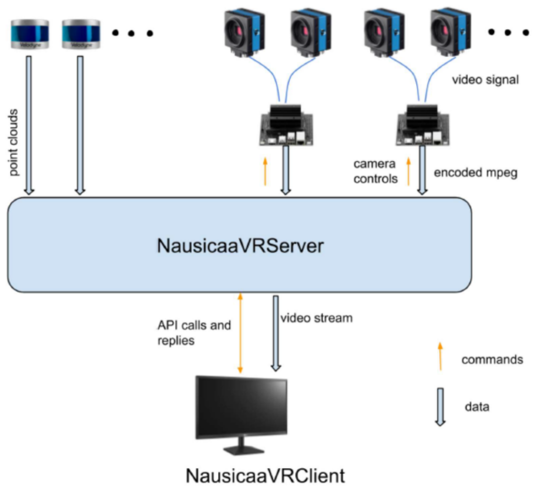

Figure 1: Hardware-Software System

The schematic diagram 1 represents a broad overview of our framework as a whole. The following section 3.1 and 3.2 provide a detailed description of our framework including the hardware configuration followed by the proprietary software interface. The hardware is a multi-modal sensor system consisting of two Lidar scanners and four embedded color cameras mounted with fish-eye lenses. The lidar scanners are Velodyne (VLP-16 PUCK LITE) and cameras from the Imaging source (ImagingSource, 2017) designed to be used in harsh environments.

3.1 Hardware Configuration

The cameras are connected to NVIDIA Jetson embedded hardware driven by Linux Tegra OS. Jetson's hardware (Nvidia, 2017) along with its SDKs supports Artificial Intelligence (AI) products and is ideal for autonomous machines and other integrated applications. The video signal from the cameras is encoded into the H264 stream and transmitted over a wired network to the server.

The hardware acceleration support from the Jetson provides fast encoding of the video stream and is capable of transmitting HD-resolution data at 60fps. The sensor parameters for each individual camera are manually refined based on the information from the camera SDK and are highly dependent on the acquisition environment. Furthermore, H264 encoding and streaming parameters are fine-tuned according to the specifications of hardware encoding acceleration supported by Nvidia Jetson. The camera sensor and its corresponding data stream encoding parameters are combined using an open-source multimedia framework (GStreamer) pipeline to transmit data as UDP packets. The individual lidars (VLP-16) stream the 3D point data as UDP packets via ethernet in real-time. Additionally, an Intel core-i9 PC with Nvidia GeForce RTX 3090 graphics card (24GB) running on Windows 11 Platform receives UDP packets from each individual sensor for further processing and visualization.

3.2 Software Configuration

The streamed data from the lidars and cameras are further processed and visualized in our proprietary application framework. The framework primarily supports real-time rendering of lidar point clouds, visualization of the camera streams, lidar-lidar alignment, and camera-lidar alignment. The geometry from the 3D point cloud and texture from the camera images are mapped utilizing the alignment information to generate a realistic rendered view of the surroundings. We also facilitate remote visualization of the rendering based on MJPEG streaming on a web browser. Additionally, communication between a client application and a Server PC is supported through network socket connection and API functionalities. It allows the client to communicate with the application running on a server PC to virtually render the scene by positioning a virtual camera at multiple locations while also receiving essential feedback.

4 REGISTRATION OF LIDARS AND RGB CAMERAS.

The problem of calibration with Velodyne VLP16 is fairly well-known. The bulk of the literature, as for exmaple (An et al., 2020; Park et al., 2014; Li et al., 2022) revolves around the problem of establishing 3D-2D correspondences between the point cloud provided by the LIDAR and the image from the RGB cameras. The difficulty of this problem depends on a few factors.

- the resolution of the LIDAR. We need to determine the 3D position of a target point that, in general, is not directly sampled but must be inferred by the point cloud. The more the latter is sparse, the more difficult it is to find the target point.
- the disposition of camera and LIDAR. Since the target point need to be seen both from the LIDAR and the camera, their relative position influences the sparsity of the point cloud. For example, if the camera is distant from the LIDAR and points away from it (as it usually is in practical situations) the sampling on the target will be more sparse.
- the surrounding environment. If LIDARs and cameras are in a controlled environment we can build ad-hoc configurations to make the correspondences finding easier. For example, in an empty room, we could use the corner points at the intersection of walls and floor (or ceiling).

Unfortunately, our typical scenario is ill-conditioned with respect to all the factors listed above: the VLP16 has a poor resolution in the vertical axis and poor precision on depth values, the cameras and LIDARs may be placed several meters away and the calibration may be needed to be done with the boat on the water, with literally nothing around. With these difficulties in mind, we tried to develop an ad-hoc target that could be easily carried and still large enough to be detected at a distance, as explained in the following section.

4.1 Creating the calibration target

Our goal was to create a physical target that could be reliably and automatically recognized from the point cloud and on the images, easy to be physically built and light to be held even from an off-the-shelf commercial drone. The first prototype was a cusp defined by the intersection of three non-coplanar planar pieces of cardboard as shown in Figure 2 (left). A similar idea was proposed in (Bu et al., 2021). The rationale behind this choice is that even an incomplete sampling of the three planar regions would define their supporting planes and hence the cusp point (as the intersection of the supporting planes). However, although the method worked, we found that the detected cusp point was not very accurate even at a not-so-distant position. This is because the precision of the LIDAR values is such that the planar fitting of a relatively small region of space (around 100 points) may result in a "range" of equally valid fitting planes and therefore their intersection defines a point in a radius of several centimeters even at just 3 meters from the LIDAR.

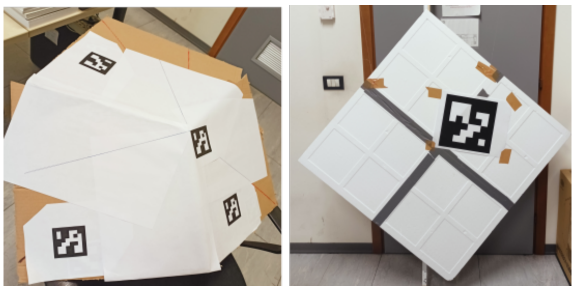
Figure 2: Left: an early version of the target; Right: target used with our system.

Our target is designed to harness the scan directions where the LIDAR is most precise,i.e, the azimuthal direction while being robust against vertical low-frequency sampling and lack of precision in the depth measurement.

We use a simple $1m \times 1m$ square which is hung by a corner and take its center as the target point (right side of Figure 2). Figure 3 shows an example of how the point cloud appears. We then apply the following few simple steps:

1. fit a plane on the sampling points of the square
2. project the points on the fitted plane
3. rotate the projected point cloud on the plane to minimize the size of the (2D) bounding box
4. if the size of the bounding box is within tolerance from the expected size of $1m \times 1m$ then the center of the bounding box is the target

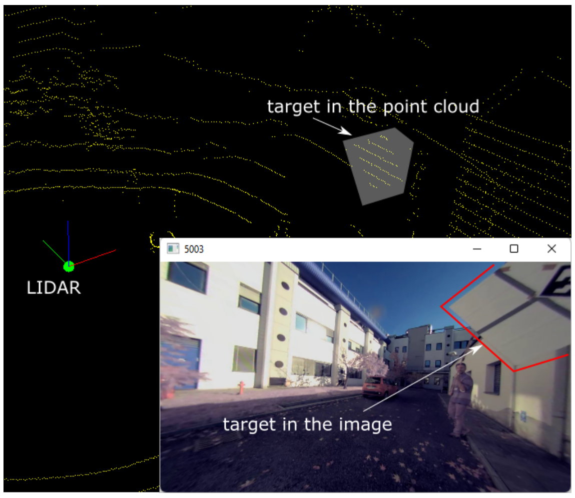

Figure 3: Example of how the target appears in the point cloud and in one of the RGB images.

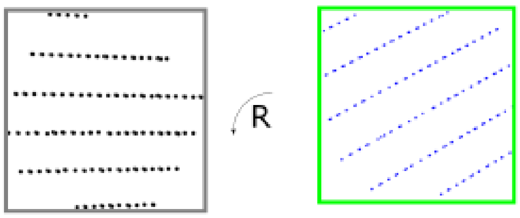

Figure 4: Left: Points on the target projected on their fitting plane. Right: Point rotated to fit the (known) bounding box of the target.

The described algorithm essentially performs a fitting of a fixed-size square on the point cloud, using the bounding box as a cost function. Note that, in its simplicity, this method has two useful qualities. It only needs a partial sampling of the points along the sides in order to be detected. It is tolerant to errors in depth measurement. This latter statement can be supported by sketching a simple proof. Let us consider the scheme in Figure 5 showing the 2-dimensional case. The actual supporting line (that is, the actual plane of the target) is $\mathbf{L}$ but because of the imprecise depth values, we fit the point with line $\mathbf{L}_f$. Let h be the thickness of the slab of points that are supposed to be on the same line. We can find the angle between the worst fitting line $\mathbf{L}_F$ and $\mathbf{L}$ as $\alpha_{err} = arctan(h/0.5)$. It follows that the projection of the point on this line will be erroneously scaled by $cos(\alpha_e rr)$, that is $\|p_f\| = \|p\| * cos(\alpha_{err})$. Now, to put things in perspective, consider that at 4 meters from the LIDAR, we can have a depth error around $0.03m$, which gives an error of $cos(arctan(0.03/0.5)) = 0.998$, which means that we can have the square shrunk at most by $2mm$.

Detecting the same target in the RGB images is an easier problem which is solved with consolidated

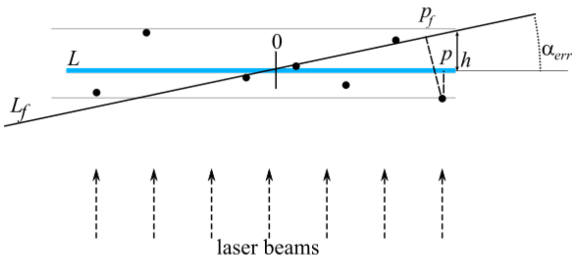

Figure 5: Proof sketch that approximated depth measurement has limited effect on the computation of the target size.

markers such as the Aruco markers (Garrido-Jurado et al., 2014).

4.2 Calibration procedure

The calibration procedure requires showing the target to the LIDARs and cameras until enough correspondence is collected to align the data. At startup, the user is required to hint at the region of the point cloud containing the target with a simple mouse click. The target is then continuously tracked in the point clouds. Every time the target is found in both point clouds, a new 3D-3D correspondence is collected and it will be used to align the point clouds. If the target is found in at least one point cloud, then its 2D counterpart is looked for in the images. For each image where the target point is found, a 3D-2D correspondence is added. In principle, we need only 4 3D-3D correspondences in order to align the point clouds and only 4 3D-2D correspondences for each of the images. However, in both cases, the quality of the alignment heavily depends on the accuracy and distribution of the correspondences. For instance, quasi-collinear 3D points will result in unreliable point cloud alignment. Likewise, 2D points concentrated in a small region of the image will produce an incorrect result. Therefore, the simple algorithm described above needs further details.

Acquisition time. Since we have multiple sources of data that are asynchronously collected, we cannot guarantee that they were acquired at the same time and in general, aren't. This is a problem when the target is moving because we would obtain the wrong correspondence. Therefore we compute the target speed and use its position only when it moves extremely slowly (5cm/s in our experiments). Also, we check the arrival time of point clouds and data and discard the correspondences if the time between the point cloud/images they were found in is over a threshold (100ms in our experiments).

Distribution of correspondences. Both for 3D-3D and 3D-2D alignments, we need a sparse set of correspondences. Furthermore, we need that they are not close to degenerate configurations, which means collinear (for both types of alignments) or that the 3D points are on the same plane (just for 3D-2D alignment). We use progressive Poisson Sampling (Corsini et al., 2012). Starting with a large disk radius R, we look for 4 samples that are at least R units apart. If they are found, we look that they are not in a degenerate configuration. If they are not found, we reduce R by $1/10$ and repeat until they are found or the process fails. Figure 6 shows an example of points selection in one of the RGB frames

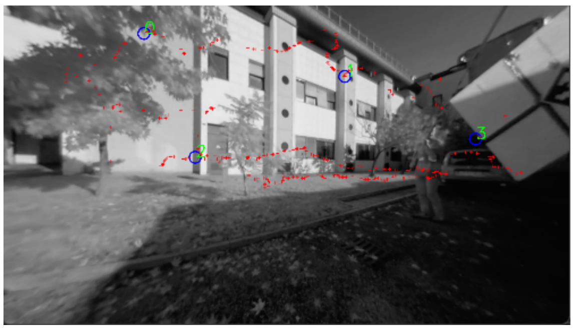
Figure 6: All the correspondences found between the image and the 3D geometry as red dots. Selected correspondences are rendered with blue circles. The greyscale version of the image is rendered in order to better highlight the correspondence points

5 ON-THE-FLY ACQUISITION AND RENDERING FROM LIDAR AND RGB CAMERAS.

The overall system as described in section 3 is adapted in our experiments to acquire multi-sensor data and render the scene in real-time. LIDARs and RGB camera feeds are combined at run-time to offer a free point-of-view rendering. This is done by on-the-fly tessellation of point clouds and projective mapping, detailed below.

Tessellation of the point clouds Defining a 2D surface from a point cloud is a longstanding problem and several different solutions have been proposed over the years (please refer to (Berger et al., 2017) for a survey on this topic). The characteristics that make the problem difficult are sparsity and uneven sampling, forcing the solver to make some assumptions about the nature of the sampled surface. However, in the specific case of LIDARs, sampling is partial but locally dense and structured on a grid, which makes it possible (and reasonable) to use a predefined regular tessellation of the points Note that all of the above does not require any processing on the CPU side, the data arriving from the LIDARs are sent to the GPU as vertices, the tessellation pattern is static and for filtering the triangles we use a geometry shader that discards the unwanted triangles.

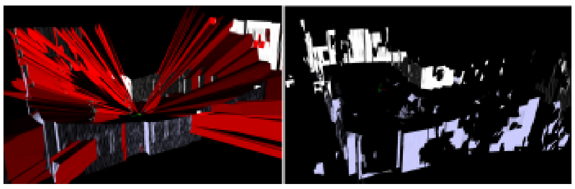
Figure 7: Elongated triangles (in red) usually connect portions of surfaces that are disconnected/different and hence automatically removed. The Left and right images show the same data before and after removal of triangles.

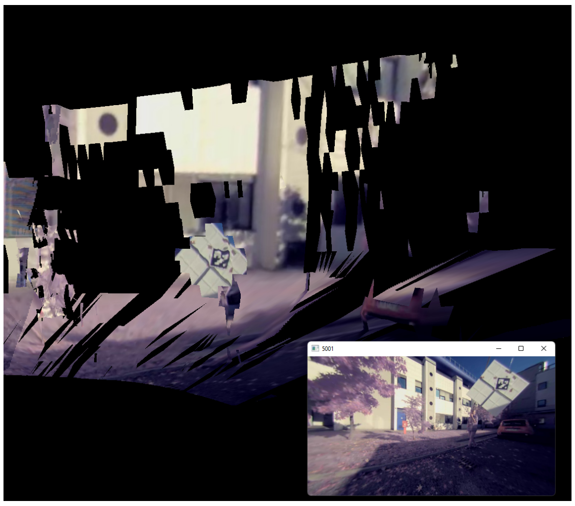

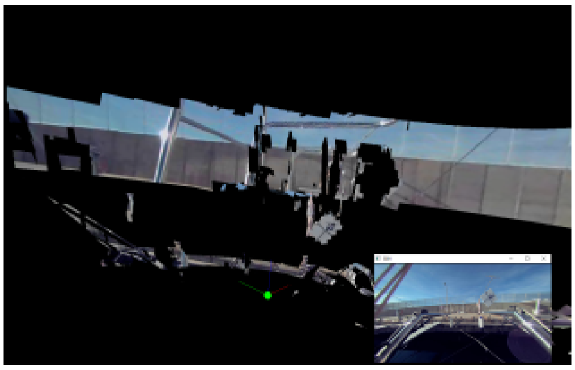
Figure 8: Snapshots of the textured geometry. The camera feed is also shown at the bottom.

Projecting RGB images The final color of the geometry is obtained by means of projective texturing (NVidia, 2001). This requires a first rendering pass where, for each camera, a shadow map is created and used in the rendering pass to see from which cameras each point is visible. Please note that, typically, there are regions of space that are covered by multiple cameras, therefore we need an efficient way to combine the, usually different, contributions in a reasonable way. We use the technique presented in (Callieri et al., 2008) which consists of blending the contribution of each camera according to the cosine of the angle of the projection direction with the surface normal. Furthermore, we apply an image equalization step based on histogram matching (Pizer et al., 1987) for a better blending of images in overlapping regions.

Remote Rendering The tessellated point cloud followed by projective texturing based on the camera vantage point generates a realistic rendering of the environment. The rendering data is directly read from the GPU (framebuffer) and parsed as a stream of jpeg images strictly maintaining the quality of the rendered output. The remote rendering is facilitated by a separate MJPEG streaming network socket connection apart from our usual client-server communication. The MJPEG-encoded videos are then sent over HTTP protocols using an easily integrable multi-threaded and computationally inexpensive streaming framework allowing clients to remotely visualize real-time rendered content on a web browser. Besides the MJPEG streaming, our application also supports visualization of the rendered content as H264 streams over real-time streaming protocol(RTSP) using FFMPEG library (Tomar, 2006).

6 CONCLUSION

We presented a system for real-time acquisition and rendering of 3D scenes using low-cost LIDARs and RGB cameras, dubbed NausicaaVR. NausicaaVR supports semi-automatic calibration, on-the-fly tessellation, and remote rendering and is built with a client-server architecture. A possible direction of improvement is the rendering of the reconstructed scene. Although the results of our system were satisfactory for the goal of environmental awareness, the regular tessellation of the data creates several rendering artifacts, especially due to unsampled regions that cause part of the images to be projected on the background. One viable solution would be not to use the geometry as it is but as a proxy to place impostors,i.e, basic primitive shapes onto which to project texture. However, the use of impostors should be combined with real-time segmentation of the images in order to avoid pixels belonging to the background (e.g. the sky) being projected into such impostors. Another avenue for research is to use 3D data from multiple frames. With the current solution, each frame is rendered as is but instead we could cumulate the point clouds from multiple frames for creating a more complete geometry. However, since the boat is not steady, we would need its position and orientation to place the data in a common reference system, that is, to compensate for the motion and rotation. This information could be obtained by using an IMU sensor, which unfortunately was not available at this time.

ACKNOWLEDGEMENTS

This work was supported by the project NAUSICAA - NAUtical Safety by means of Integrated Computer-Assisted Appliances 4.0 (DIT.AD004.136)

REFERENCES

An, P., Ma, T., Yu, K., Fang, B., Zhang, J., Fu, W., and Ma, J. (2020). Geometric calibration for lidar-camera system fusing 3d-2d and 3d-3d point correspondences. *Opt. Express*, 28(2):2122–2141.

Berger, M., Tagliasacchi, A., Seversky, L. M., Alliez, P., Guennebaud, G., Levine, J. A., Sharf, A., and Silva, C. T. (2017). A survey of surface reconstruction from point clouds. In *Computer Graphics Forum*, volume 36, pages 301–329. Wiley Online Library.

Brinkmann, M. and Hahn, A. (2017). Testbed architecture for maritime cyber physical systems. In *2017 IEEE 15th International Conference on Industrial Informatics (INDIN)*, pages 923–928.

Bu, Z., Sun, C., Wang, P., and Dong, H. (2021). Calibration of camera and flash lidar system with a triangular pyramid target. *Applied Sciences*, 11(2).

Callieri, M., Cignoni, P., Corsini, M., and Scopigno, R. (2008). Masked photo blending: mapping dense photographic dataset on high-resolution 3d models. *Computer & Graphics*, 32(4):464–473. for the online version: http://dx.doi.org/10.1016/j.cag.2008.05.004.

Corsini, M., Cignoni, P., and Scopigno, R. (2012). Efficient and flexible sampling with blue noise properties of triangular meshes. *IEEE Transactions on Visualization and Computer Graphics*, 18(6):914–924.

dspace (2021). `https://www.dspace.com/en/pub/home/applicationfields/stories/smartkai-parking-assistance-f.cfm`.

Garrido-Jurado, S., Muñoz-Salinas, R., Madrid-Cuevas, F., and Marín-Jiménez, M. (2014). Automatic generation and detection of highly reliable fiducial markers under occlusion. *Pattern Recognition*, 47(6):2280–2292.

Hahn, T., Damerius, R., Rethfeldt, C., Schubert, A. U., Kurowski, M., and Jeinsch, T. (2022). Automated maneuvering using model-based control as key to autonomous shipping. *at - Automatisierungstechnik*, 70(5):456–468.

ImagingSource (2017). `https://www.theimagingsource.com`.

Kim, H., Kim, D., Park, B., and Lee, S.-M. (2020). Artificial intelligence vision-based monitoring system for ship berthing. *IEEE Access*, 8:227014–227023.

Li, Q., Queralta, J. P. n., Gia, T. N., Zou, Z., and Westerlund, T. (2020). Multi-sensor fusion for navigation and mapping in autonomous vehicles: Accurate localization in urban environments. *Unmanned Systems*, 08(03):229–237.

Li, X., He, F., Li, S., Zhou, Y., Xia, C., and Wang, X. (2022). Accurate and automatic extrinsic calibration for a monocular camera and heterogenous 3d lidars. *IEEE Sensors Journal*, 22(16):16472–16480.

Martelli, M., Virdis, A., Gotta, A., Cassarà, P., and Di Summa, M. (2021). An outlook on the future marine traffic management system for autonomous ships. *IEEE Access*, 9:157316–157328.

NVidia (2001). `https://www.nvidia.com/en-us/drivers/Projective-Texture-Mapping/`.

Nvidia (2017). Nvidia announces jetson tx2: Parker comes to nvidia's embedded system kit.

Paneque, J., Valseca, V., Martínez-de Dios, J. R., and Ollero, A. (2022). Autonomous reactive lidar-based mapping for powerline inspection. In *2022 International Conference on Unmanned Aircraft Systems (ICUAS)*, pages 962–971.

Park, Y., Yun, S., Won, C. S., Cho, K., Um, K., and Sim, S. (2014). Calibration between color camera and 3d lidar instruments with a polygonal planar board. *Sensors*, 14(3):5333–5353.

Perera, L., Moreira, L., Santos, F., Ferrari, V., Sutulo, S., and Soares, C. G. (2012). A navigation and control platform for real-time manoeuvring of autonomous ship models. *IFAC Proceedings Volumes*, 45(27):465–470. 9th IFAC Conference on Manoeuvring and Control of Marine Craft.

Pizer, S. M., Amburn, E. P., Austin, J. D., Cromartie, R., Geselowitz, A., Greer, T., ter Haar Romeny, B., Zimmerman, J. B., and Zuiderveld, K. (1987). Adaptive histogram equalization and its variations. *Computer vision, graphics, and image processing*, 39(3):355–368.

Rüssmeier, N., Hahn, A., Nicklas, D., and Zielinski, O. (2016). Ad-hoc situational awareness by optical sensors in a research port maritime environment , approved networking and sensor fusion technologies.

Schiaretti, M., Chen, L., and Negenborn, R. R. (2017). Survey on autonomous surface vessels: Part i - a new detailed definition of autonomy levels. In Bektaş, T., Coniglio, S., Martinez-Sykora, A., and Voß, S., editors, *Computational Logistics*, pages 219–233, Cham. Springer International Publishing.

Schubert, A. U., Kurowski, M., Gluch, M., Simanski, and O Jeinsch, T. (2018). Manoeuvring automation towards autonomous shipping. Zenodo.

Snyder, F. D., Morris, D. D., Haley, P. H., Collins, R. T., and Okerholm, A. M. (2004). Autonomous river navigation. In *SPIE Optics East*.

Thombre, S., Zhao, Z., Ramm-Schmidt, H., Vallet García, J. M., Malkamäki, T., Nikolskiy, S., Hammarberg, T., Nuortie, H., H. Bhuiyan, M. Z., Särkkä, S., and Lehtola, V. V. (2022). Sensors and ai techniques for situational awareness in autonomous ships: A review. *IEEE Transactions on Intelligent Transportation Systems*, 23(1):64–83.

Tomar, S. (2006). Converting video formats with ffmpeg. *Linux Journal*, 2006(146):10.

Wright, R. G. (2019). Intelligent autonomous ship navigation using multi-sensor modalities. *TransNav, the International Journal on Marine Navigation and Safety of Sea Transportation*, 13(3):503–510.